Temperature-Dependent Tunneling in Furan Oligomer Single-Molecule Junctions

Haipeng B. Li,[†, ‡,#] Yan-Feng Xi,[†,#] Ze-Wen Hong,[⊥,] Jingxian Yu,[§] Xiao-Xia Li,[†] Wen-Xia Liu,[†] Lucas Domulevicz,[‡] Shan Jin,[*, †], Xiao-Shun Zhou,[*, ⊥] and Joshua Hihath,[*, ‡]

[†] Key Laboratory of Pesticide and Chemical Biology, Ministry of Education, College of Chemistry, Central China Normal University, Wuhan 430079, China

[‡]Department of Electrical and Computer Engineering, University of California Davis, Davis, California 95616, United States

[⊥] Zhejiang Key Laboratory for Reactive Chemistry on Solid Surfaces, Institute of Physical Chemistry, Zhejiang Normal University, Jinhua, Zhejiang 321004, China

[§]ARC Centre of Excellence for Nanoscale BioPhotonics (CNBP), Institute for Photonics and Advanced Sensing, Department of Chemistry, The University of Adelaide, Adelaide, SA 5005, Australia

KEYWORDS: molecular electronics; charge transport; thermally assisted tunneling; furan-based molecular wire; single-molecular conductance; single-molecule break junction

ABSTRACT:

Two commonly observed charge transport mechanisms in single-molecule junctions are coherent tunneling and incoherent hopping. It has been generally believed that tunneling processes yield temperature-independent conductance behavior and hopping processes exhibit increasing conductance with increasing temperature. However, it has recently been proposed that tunneling can also yield temperature-dependent transport due to the thermal broadening of the Fermi energy of the contacts. In this work, we examine a series of rigid, planar furan oligomers that are free from a rotational internal degree of freedom to examine the temperature dependence of tunneling transport directly over a wide temperature range (78 K to 300 K). Our results demonstrate conductance transition from a temperature independent regime to a temperature dependent regime. By examining various hopping and tunneling models and the correlation between the temperature dependence of conductance and molecular orbital (MO) energy offset from the Fermi level we conclude thermally assisted tunneling is the dominant cause for the onset of temperature dependent conductance in these systems.

Various oligomers have received significant attention during the past decade as potential candidates for single-molecule devices.[1–3] In the vast majority of these devices the transport has been ascribed to one of two charge transport mechanisms, either tunneling or hopping.[4] These regimes are often distinguished by measuring the temperature dependence of the molecular conductance. Generally, temperature-independent transport has been equated to a tunneling process[5,6] and temperature-dependent transport has been assumed to be a hopping process[7]. However, various recent studies have observed conductance trends deviating from the prediction of a simple charge transport model. Specifically, the temperature-independent tunneling model predicts the exponential decay as the oligomer number increases, meanwhile studies have observed the deviation from the exponential decay trend.[8–11] It has been suggested that this deviation is due to a transition from tunneling to hopping mechanisms[8,9], while others suggest that it is a thermal excitation of the dihedral bonds within the molecule that improves the π-coupling[10,11]. A third possibility is that the thermal broadening of the Fermi energy in the electrodes leads to the observed temperature dependence of the molecular conductance[12,13]. In the studies to date, the rotational freedom of the molecule under combined with the limited temperature range in the measurement system has limited the ability to disambiguate between these possible mechanisms.

In the presented work, we design and synthesize a series of rigid, structurally well-defined planar furan oligomers **F1**-**F8** (corresponding to 1 to 8 furan units, Figure 1) to determine if the proposed thermally assisted tunneling process can be observed in a single-molecule system. The molecular structure creates a large energy-barrier for rotation of the furan groups (>10 eV for a moderate 10° angle, see Figure S3), practically eliminating rotational movement within the molecular chain and ensuring conjugation throughout the system (Figure 4b), which makes a thermally activated rotational movement extremely unlikely.[10] This strong coupling between the furan groups

drastically reduces the probability of hopping between adjacent units allowing study of thermally induced conductance changes in a coherent system. To perform the studies a single-molecule break junction (SMBJ) system is integrated into a cryostat providing a wide temperature range (78 K to 300 K), and thus allowing differentiation of Fermi-broadening induced temperature dependence from other thermally activated charge transport mechanisms[14]. The molecular structures and electronic properties of these molecular junction devices are further elucidated by combining density functional theory (DFT) with the non-equilibrium Green's function (NEGF). This thermally assisted tunneling is a coherent process which is fundamentally different from a hopping process.[15] And the ability to modulate temperature dependence of a series of single molecule chains provides further possibilities in designing functional molecular electronics system.

EXPERIMENTAL SECTION

Chemicals and Synthesis.

All solvents were pre-dried, distilled, and degassed prior to use. CH_2Cl_2 was distilled from P_2O_5, and tetrahydrofuran (THF) was freshly distilled from Na/benzophenone under nitrogen atmosphere. Other chemical reagents were of analytical grade and used without further purification unless otherwise stated. The furan-based molecular wires **F1**-**F8** were prepared following the procedures described in the Supporting information. All reactions were carried out using standard Schlenk techniques under a high purify argon atmosphere.

Room temperature SMBJ system (RT-SMBJ)

Prior to each experiment, Au (111) substrate was electrochemically polished and annealed in a hydrogen flame. After naturally cooled in N_2, Au (111) was immersed in freshly prepared

dichloromethane containing 0.1 mM target molecule for 10 min, then dried in nitrogen gas, and measured in decane in ambient conditions. All the experiments were performed in a modified Nanoscope IIIa STM (Veeco, US) by using STM break junction (STM-BJ).[16–19] The conductance measurements start by moving the tip into the substrate to create a metal point-contact. Then the tip is withdrawn from the substrate at a speed of 20 nm/s, and the current is recorded at a fixed bias. We measured all **F1** to **F8** furan molecules with RT-SMBJ system and ~ 2000 traces are collected to construct conductance histogram without data selection. The datasets are shown in Figure 1c-d as well as red squares in Figure 2a.

SMBJ system with cryostat (cryo-SMBJ)

The low temperature SMBJ experiment is performed with a lab-designed STM head controlled by lab-developed LabView control and data collection application. STM tips are prepared with high purity Au wire (Alfa Aesar, 99.998% purity). The gold substrate is made with a mica substrate (Ted Pella) freshly cleaved in a cleanroom and deposited with 130 nm gold (99.999 % purity, Kurt J. Lesker) E-Beam evaporator. The sample under test is prepared through a self-assembled monolayer (SAM) on top of a gold substrate. Saturated furan solution in THF (98% purity, Sigma-Aldrich) which the gold substrate is submerged to overnight (~ 16 hrs) is used to prepare SAM for SMBJ test. The gold substrate with SAM is then dried with high purity nitrogen right before the experiment, placed onto the SMBJ head and loaded into the cryostat chamber (Janis Research Co.) and the system is pumped down to ~10^{-6} Torr. Liquid nitrogen (Airgas) filled the cryostat cools the system to 78 K, and resistive heaters on the cold plate could maintain the STM head temperature between 78 K and 300 K. The process for performing SMBJ experiments is the same as described above. With this cryo-SMBJ setup, we carried out low temp conductance measurements (Figure 2a, dark blue squares) as well as all the temperature dependence

conductance trend measurement (all the data points Figure 2b) for **F4-F6** with Au contacts and **F5** with Pt contacts.

RESULTS AND DISCUSSION

Electronic Characterization at Room Temperature. A schematic setup of a SMBJ experiment is shown in Fig. 1b. An STM based SMBJ system is used to measure the conductance of **F1** to **F8** at 300 K. Furan molecules are self-assembled on top of one gold contact in solvent and the other gold electrode repeatedly approaches and retracts from the gold surface. A constant DC bias is applied between the two electrodes. During the retraction process, the current is recorded as a function distance *d* and translated into conductance. Once an Au-molecule-Au junction is formed, a clear step in the typical semi-logarithmic conductance traces ($\log(G/G_0)$, $G_0=2e^2/h$) versus the relative electrode displacement (d) can be observed (Figure 1c). All conductance versus distance traces collected for each molecule in the SMBJ setting are added to a histogram to determine the most probable conductance value. As shown in Figure 1d, the most probable conductance value is determined by a Gaussian fitting (grey curves) of the conductance peak.

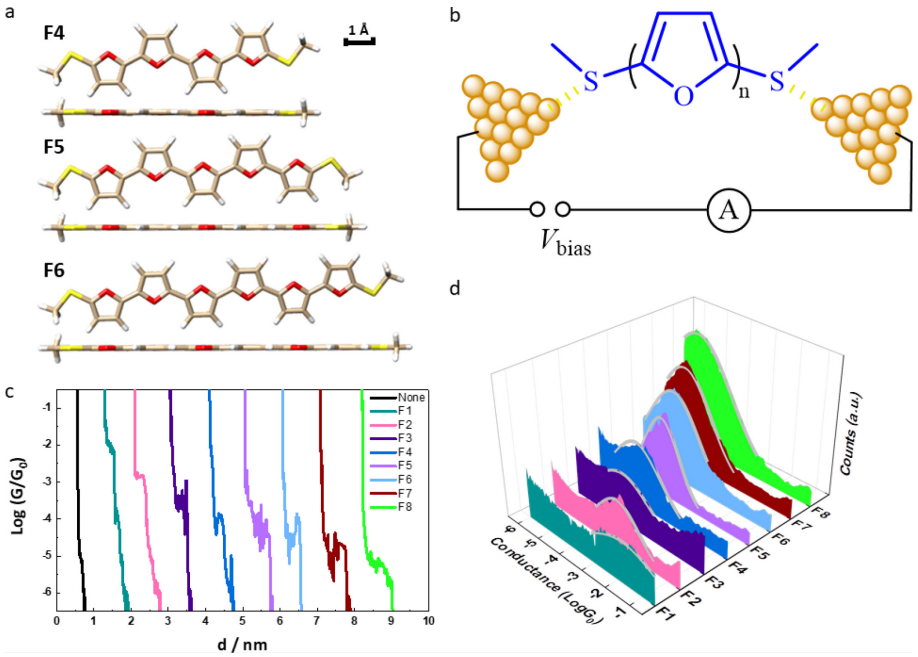

Figure 1. (a) Example of furan optimized structures for **F4-F6** (n = 4-6) based on DFT calculations. The side view of the structures demonstrates the planar nature of the molecules. (b) Schematic setup of the SMBJ experiment. A constant bias is applied to the molecular junction and the current is monitored during the pulling process. (c) Single molecule conductance versus distance traces obtained during an SMBJ experiment at 300 K (RT-SMBJ). The black curve represents pulling an Au-Au junction where no molecule binds to the electrodes. Traces are offset horizontally for clarity. (d) Conductance histograms for **F1** to **F8** based on ~ 2000 conductance traces for each furan molecule chain without selection collected in this RT-SMBJ system. The amplitudes of the peaks are scaled arbitrarily to give a clear view. Grey curves are Gaussian peak fitting for each histogram to determine the most probable conductance.

The extracted conductance values at 300 K from Figure 1d are summarized in Figure 2a as red data points as a function of molecular length; each data point is from three tests based on three freshly prepared SAM samples and the error bar is smaller than the size of the data point in the figure. As shown in Figure 2a, from molecular wire **F1** to **F4**, the conductance vs. length follows a clear exponential decay with a decay constant β = 4.4 nm^{-1}, suggesting that temperature-

independent tunneling is the dominant transport mechanism[20]. However, once the number of furan units in the oligomer is greater than 4, the conductance deviates from the exponential decay trend observed for shorter molecules, suggesting that a thermally activated charge transport mechanism potentially gives an additional contribution to the conductance of the molecular junction at higher molecule lengths.

Temperature Dependence. To verify this hypothesis, we used a temperature-controlled SMBJ system to perform SMBJ experiments in a low temperature (78 K) and high-vacuum (10^{-6} Torr) environment. We overlay the conductance values for **F4**-**F6** at 78 K measured via cryo-SMBJ system (blue squares) on top of the 300 K conductance measured via RT-SMBJ system in Figure 2a. As indicated by the dashed line, at a low temperature (78 K), **F5** and **F6** follow the same exponential decay trend as the shorter molecule conductance at 300 K suggesting that the conductance is dominated by tunneling at 78 K for **F5** and **F6**. A transmission spectrum generated from a DFT simulation and non equilibrium Green's function transport calculation demonstrating this exponential decay trend is in the Supporting Information (Figure S4). Meanwhile, the temperature dependence of the conductance of **F5** and **F6** also proves that a thermally activated conductance component starts to contribute at an elevated temperature.

To quantitatively study this thermal contribution, we perform a series of conductance measurements for **F4**-**F6** over a wide temperature range (78 K to 300 K). The results are presented as $\log(G/G_0)$ vs. 1/T plots in Figure 2b. For the **F4** molecule, the conductance value is almost a constant throughout the temperature range, suggesting that the thermal contribution is playing a minor role for the shorter furan molecules. However, for **F5** and **F6**, we observe two conductance regimes with different temperature-dependence: a temperature-independent regime (< 266.2 K for **F5** and < 248.7 K for **F6**) and temperature-dependent regime above these values (Figure 2b).

Thermally activated transport. Conventionally, the assumption is that temperature-dependent conductance behavior indicates a hopping mechanism[7,21]. However, there have been several theoretical works and experimental observations suggesting that thermally assisted tunneling can also lead to a significant temperature dependence[12,13]. A schematic description of thermally assisted tunneling is shown in Figure 2c. In a thermally assisted tunneling model the temperature dependence originates from the fact that the Fermi-Dirac distribution of electrons in the leads is a function of temperature, and that as the temperature increases there will be more charge carriers closer to the dominant molecular orbital, which we note is different from conformational changes leading to a temperature dependence.[21–23] As shown in Figure 2c, at low temperatures (blue curves), only a small number of electron states near the HOMO level of the molecule are available in the leads which can contribute to the tunneling process. However, at an elevated temperature (red curves in Figure 2c), a broadened Fermi-Dirac distribution generates more empty states near the HOMO level, some of which can be close to resonance, which leads to an increase in the transmission probability, and thereby the conductance. This thermally assisted tunneling mechanism is different from a hopping transport since the charge carrier is still transporting through a coherent tunneling process, whereas in a hopping process the charge carrier physically occupies the molecule before exiting, which is a multi-step process. Relaxation during this process causes the electron to lose coherence. To proceed, we consider each model independently to determine the conduction mechanism for the longer furan molecules at elevated temperatures.

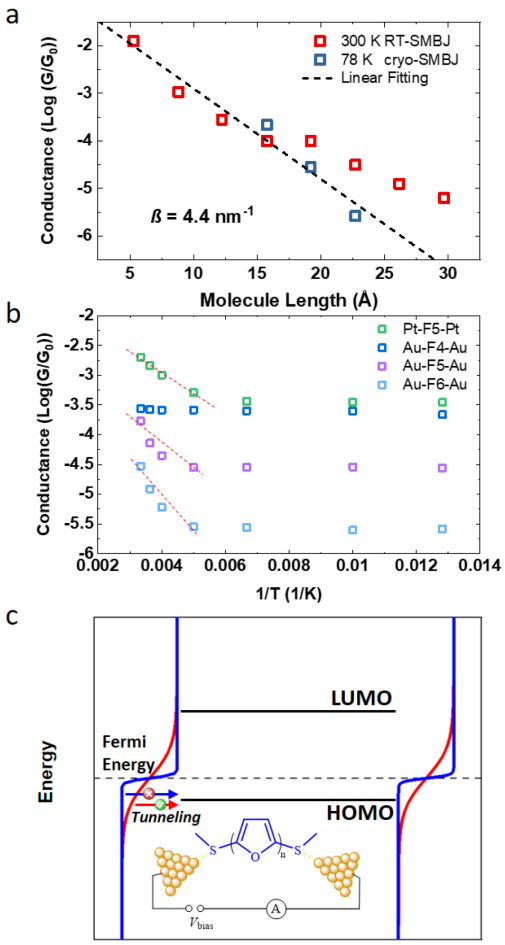

Figure 2. Temperature and length dependence of the furan molecules. (a) Conductance vs. molecule length at 300 K (red square via RT-SMBJ) and 78 K (blue square via cryo-SMBJ). Dashed line is a linear fitting of the conductance in the temperature-independent regime. (b) Temperature dependence of the conductance for **F4**, **F5**, and **F6** (log(G/G$_0$) vs. 1/T). For Au contacts, **F4** does not show obvious temperature dependence which suggests temperature independent tunneling. **F5** and **F6** exhibit two regimes: a temperature-dependent regime ($T > T_C$) and a temperature-independent regime ($T < T_C$) (T_C summarized in Table 1). For Pt contacts, **F5** also demonstrates temperature dependence. Red dashed lines are a guide to the eye. (c) Schematic plot of thermally assisted tunneling model. Blue curves and red curves correspond to low temperature and high temperature density of states (DOS) of the electrons. Electrons from the left leads could tunnel through the junction in a single step to the right lead where empty states are available at an elevated temperature (red curves). Meanwhile at a low temperature, minimum

empty states from the lead near HOMO level therefore the tunneling current near HOMO level is minimized (blue curves).

To assess the thermally assisted tunneling mechanism, we adopt a model developed by Baldea et al.[13], as shown in Equation 1.

$$G = G_{0K} + G_T = G_{0K}\left(\frac{\varepsilon_0}{\Delta};\Delta\right) + D(\Delta)\frac{\mathrm{sech}^2\frac{\varepsilon_0}{2k_BT}}{k_BT} \qquad (1)$$

There are two contributions of the conductance in this model. The first term G_{0K} is a temperature independent contribution which depends on the energy offset (ε_0) and the coupling coefficient (Δ) between the HOMO of the molecule and Fermi level of the gold contact. This first term corresponds to the conductance value of the molecule at 0 K, it is independent from temperature, and denoted as G_{0K}. The second term G_T is the thermally assisted tunneling conductance due to the thermal broadening of Fermi energy. D is the pre-factor, and only depends on Δ. In the temperature-dependent term, ε_0 refers to the energy offset between the HOMO of the furan oligomer and the Fermi energy of the gold contact. This ε_0 is a critical term determining how sensitive the temperature-dependence is for a specific molecular junction. For tunneling through the HOMO, we expect that **F5** has a larger ε_0 than **F6** because of the larger HOMO-LUMO gap for the shorter molecule (Figure S1 and Figure S2), which would in turn result in a different slope in the log(G/G_0) vs. 1/T plot (Figure 2b). A cross over temperature T_c is defined when the two contribution G_{0K} and G_T are equal $G_T(T)|_{T=T_c} = G_{0K}$. The fitting results of ε_0 and T_c are summarized in Table 1. Note that Equation 1 puts no restrictions on the molecule length and the two transport mechanisms represented in the two terms could coexist. However, the dominant term will shift from one to the other as the molecule length changes. Conductance of **F4** shows no obvious temperature dependence from 78 K to 300 K therefore the first term would be the

dominant charge transport mechanism. An even shorter molecule would have a larger G_{0K} and a smaller G_T due to a increased ε_0, therefore G_{0K} will always be the dominant term for **F1** to **F3** among 78 K to 300 K in this thermally assisted tunneling model. To validate this thermally assisted tunneling model we estimate the MO offset using the single-level Breit-Wigner model[24,25] and compare the results from Equation 1. This model estimates the MO offset from the *I-V* curves of the molecular junction. The equation for the model is given in Equation 2, where E_0 is the MO offset between HOMO of the molecule and Fermi level of the gold contact. Γ is the coupling between the gold electrode and the molecule from the left and the right lead. G_0 is the conductance quantum and V is the applied bias.

$$I(V) = \frac{G_0}{e}\frac{\Gamma_L\Gamma_R}{\Gamma_L+\Gamma_R}\left[\tan^{-1}\left(\frac{E_0+\frac{eV}{2}}{\frac{\Gamma_L+\Gamma_R}{2}}\right) - \tan^{-1}\left(\frac{E_0-\frac{eV}{2}}{\frac{\Gamma_L+\Gamma_R}{2}}\right)\right] \quad (2)$$

In the SMBJ experiment at 78 K, we halt the retraction process once a plateau appears in the conductance vs. time trace and sweep the bias while recording the current. By fitting the *I-V* curves with the Breit-Wigner model expressed in Eq. 2, we can estimate the MO offset denoted as E_0. We collected 30 *I-V* sweeps each for **F5** and **F6** and the results are summarized in Figure 3. The average value of extracted E_0 is expressed in Table 1.

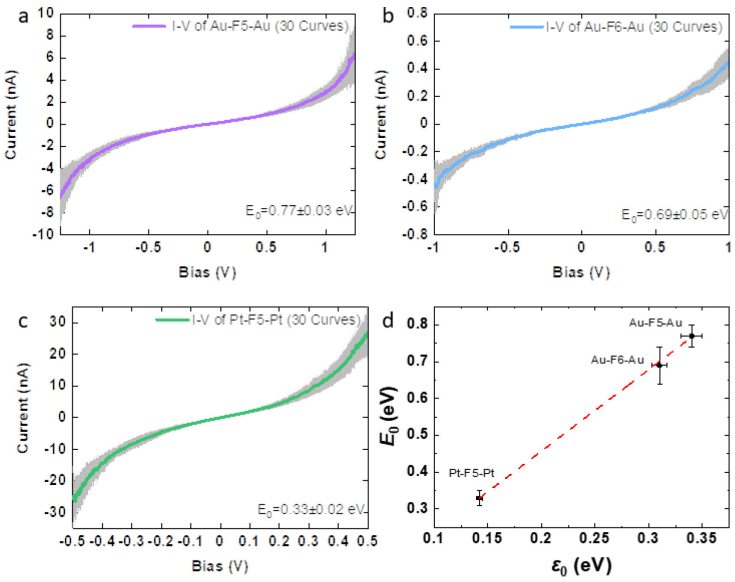

Figure 3. *I-V* characteristics for the Furan molecules. *I-V* characteristics for Au-**F5**-Au (a), Au-**F6**-Au (b), and Pt-**F5**-Pt (c) are fitted with the Breit-Wigner single level model to extract MO offset for each molecule to obtain E_0 and Γ. (d) The linear correlation between E_0 and ε_0 for all three molecular junction configurations under a thermally assisted tunneling model.

From **F4** to **F6**, we observe a decrease in E_0 which is consistent with the trend of ε_0, and the DFT calculations. Noticing that although E_0 in Breit-Wigner model implies the same physical meaning as ε_0 expressed in Eq. 1, one may not expect the observed value in the two cases to be quantitatively identical due to the different experimental conditions. In the model expressed in Equation 1, the molecular junction is under a low bias assumption: the MO energy does not change as a function of applied bias. And experimentally the molecular junction is under a constant bias of 50 mV. Meanwhile in the single-level Breit-Wigner model, a much higher bias (> 1 V) is applied in the I-V sweep. And under the high bias condition, it has been shown that the energy level of the molecule can shift by significant values[26] therefore the MO offset would not be identical between E_0 and ε_0.

To determine whether this temperature dependence is directly related to the MO offset, we also replace the gold electrodes with platinum electrodes and measure the temperature dependence (Figure 2b light green squares) as well as the *I-V* curves (Figure 3c light green curves) for Pt-**F5**-Pt junctions. Fitting with the thermally assisted tunneling model in Equation 1, for Pt-**F5**-Pt molecular junction, we extract the ε_0 based on log(G/G$_0$) vs 1/T and E_0 based on I-V sweeping curves. We plot the correlation between E_0 and ε_0 for all three molecular junctions in Figure 3d. As shown in Figure 3d, there are significant changes in the temperature dependent transport, and as such ε_0, when changing between the Au and Pt electrodes which are well correlated with the MO offset energy (E_0).

Next, to consider a thermally activated hopping model, we instead treat the system with a second model which can be expressed in terms of an Arrhenius equation. In this case, the overall conductance is given in Equation 4.[7,27]

$$G = G_{0K} + G_T = G_{0K} + Ae^{\frac{-E_A}{k_B T}} \qquad (3)$$

Again, G_{0K} is the temperature-independent tunneling component of the molecular junction. In the second term, E_A is the activation energy which is the thermal energy required for the electron to overcome the energy barrier when hopping between adjacent sites in a molecular chain. k_B is Boltzmann constant and A is a pre-factor. Fitting the log(G/G_0) vs. T data we have collected for Au-**F5**-Au, Pt-**F5**-Pt**,** and Au-**F6**-Au with Equation 3 yields E_A values that are summarized in Table 1.

At first, it appears that the hopping model can also provide a reasonable fitting to the data. In general, there are two possibilities for hopping on a molecular bridge, a multi-step hopping process along the bridge molecule, and a two-step process, where the charge moves from one electrode to

the molecule and then to the second electrode. An illustration of this multi-step hopping process is shown in Figure 4a, and the two-step process in Fig. 4c. We will consider the possibility of each of these cases based on the obtained data for activation energies, MO offsets, and coupling energies. First, for the multi-step hopping model we note that the furan molecules have a fully planar structure, and there is no thermally activated internal rotation that could be correlated with the extracted activation energy E_A that would allow site-to-site hopping within the molecule. DFT calculation demonstrates that a moderate 10-degree rotation requires an enormous amount of energy (~20 eV, Figure S3) which is not attainable in a room temperature. Previous works have used oligomers whose optimized structure is not planar. Therefore, a thermally activated twisting vibration could contribute to the temperature dependent conductance[10–12]. Once the thermal energy at the molecular junction is sufficient to activate this twisting vibration, adjacent oligomer units can rotate to the same plane to form coupled molecular orbitals and a charge can transport from one unit to another. The vibrational energy of the twisting movement should be similar to the activation energy expressed in Equation 3.[8] This value would be consistent for a molecular family, and independent of the work function of the electrodes. None of these points are true for the values extracted, so we concluded that multi-step hopping is not a likely the mechanism in our study of furan molecule.

In the case of a fully conjugated molecular system, the single-site hopping mechanism is analogous to a semiconductor quantum dot system where a single molecular orbital can be treated as a site for a charge carrier to occupy and exit the molecule.[28] In this case, it is essentially a coulomb blockade process. For this type of transport to occur, the system must be in the weak coupling regime ($\hbar\Gamma << k_BT$).[29,30] Molecules in a SMBJ configuration with physisorbed or chemisorbed anchors are often in the strong coupling regime, and in our case we have 3 experimental results

suggesting that this is the case. First, from the *I-V* curves shown in Fig. 3, and fitted using Eq. 2, we are able to extract Γ, for Au-**F5**-Au, Au-**F6**-Au, and Pt-**F5**-Pt we obtained values of 0.005 eV, 0.001 eV, and 0.007 eV respectively. All of these values are smaller than or similar to k_BT (0.007 eV at 78 K) but are within a factor of 7, which suggests we are still in the strong coupling regime. An alternative method for extracting this information is to look at the contact conductance (G_C) to the quantum dot (molecular) system. In the weak coupling regime $G_C << G_0$, and G_C can be estimated by extracting the ordinate intercept from the length dependent transport measurements (Fig. 2a). In case of the Au electrodes, we estimate G_C to be ~$0.2G_0$, which is within 1 order of magnitude of G_0, and indicative of the strong coupling regime. Finally, we can also examine the shape of the *I-V* curves themselves at low temperatures. In the weak coupling regime, there is practically zero current flow at low biases due to the very small direct coupling between the electrodes.[28,31,32] This results in an *I-V* characteristic shape similar to that shown in Fig. 4d, where the current is essentially zero until the electronic state enters the conduction window. However, as can be seen in Fig. 3, that is not the case in for the furan oligomers, here the *I-V* characteristic at 78K is continuous across the entire range, indicating significant transport probability even at low biases, and a significant coupling between the electrodes through the molecular channel (~ 2.8 nm in the case of **F6**). From these three independent pieces of evidence, we conclude that a two-step hopping mechanism is unlikely for the furan molecules, and as such the observed temperature dependence of the transport is likely due to the broadening of the Fermi function in the electrodes, and a thermally assisted tunneling mechanism.

Table 1. Summary of Parameters in a Thermally Assisted Tunneling Model vs. a Hopping Model

	Thermally Assisted Tunneling Model				Hopping Model
	ε_0 (eV)	G_{0K} (*$10^{-5}$$G_0$)	T_C (K)	E_0 (eV)	E_A (eV)
Au-**F5**-Au	0.34 ± 0.01	2.90 ± 0.10	266.2	0.77 ± 0.03	0.27 ± 0.02
Au-**F6**-Au	0.31 ± 0.01	0.27 ± 0.01	248.7	0.69 ± 0.05	0.25 ± 0.01
Pt-**F5**-Pt	0.141 ± 0.003	34.90 ± 0.10	224.5	0.33 ± 0.02	0.122 ± 0.003

[#]ε_0, G_{0K}, T_C are from fitting log(G/G_0) vs 1/T with thermally assisted tunneling model expressed in Equation 1 and Equation 2. E_0 is from fitting I-V curves with Single Level Model based on Equation 3. E_A is from fitting G vs 1/T with hopping model in Equation 4.

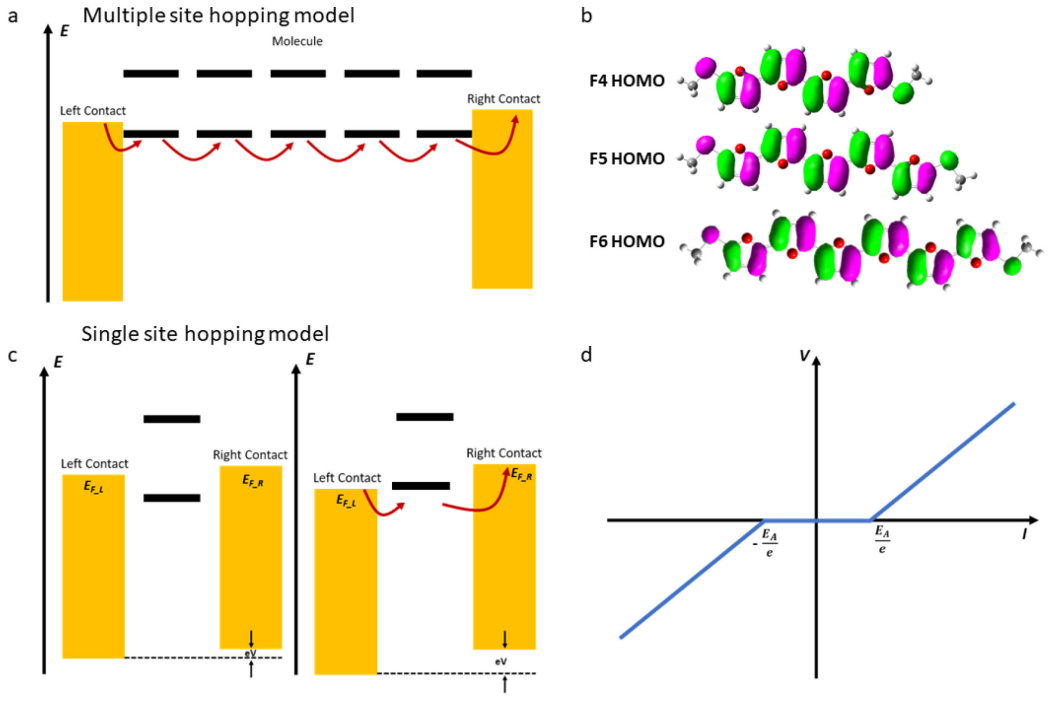

Figure 4. Hopping mechanisms. (a) Schematic of charge transport for a multi-site hopping model through the HOMO levels of bridge sites. This assumes each unit is directly coupled to adjacent sites. (b) Calculated molecular orbitals for **F4** to **F6** demonstrating a conjugated π-orbital for the HOMO with significant delocalization across the entire molecule. (c) Schematic of hopping transport through a single hopping site. (d) Schematic plot of an *I-V* curve assuming single site hopping model where the coupling between the electrodes limits current flow until an energy level enters the bias window.

CONCLUSIONS

To summarize, we have studied the conductance of a series of furan oligomers under a large temperature window and found that for the longer molecules the transport at room temperature was dominated by a thermal-transport effect. We directly examined 3 possible mechanisms for the thermally activated transport component (multi-site hopping, single-site hopping, and thermally assisted tunneling), and found that the thermally assisted tunneling model is the most consistent with the experimental observables. This result brings insight to the temperature-dependent charge transport mechanism in single-molecule junctions. The unique rigid and planar structure of the furan molecule coupled with the chemical binding to the electrodes provide a guideline for developing systems which could be both temperature dependent and still yield coherent transport properties over a long range. This study provides a new avenue for engineering molecular electronics based on the tunneling process with two different temperature dependence regimes.

ASSOCIATED CONTENT

Supporting Information

Synthesis of furan-based molecular wires **F1**-**F8**; UV-Vis electronic absorption spectra, energy optimization, and quantum transport simulations for **F1**-**F8**. This material is available free of charge via the Internet at http://pubs.acs.org.

AUTHOR INFORMATION

Corresponding Authors

Jin Shan:
jinshan@mail.ccnu.edu.cn
Joshua Hihath
jhihath@ucdavis.edu
Xiao-Shun Zhou:
xszhou@zjnu.edu.cn

Author Contributions

[#]H.L. and Y. X. contributed equally to this work.

Notes

The authors declare no competing financial interest.

ACKNOWLEDGEMENTS

The present work was supported by the National Natural Science Foundation of China (21573086, 21573198, 21872062, 21872126, and 22072053), Australian Research Council (No. CE140100003, DP180101581), the Fundamental Research Funds for the Central Universities (CCNU19TS008), and the US National Science Foundation (ECCS-1807555).

REFERENCES

(1) Garner, M. H.; Li, H.; Chen, Y.; Su, T. A.; Shangguan, Z.; Paley, D. W.; Liu, T.; Ng, F.; Li, H.; Xiao, S.; Nuckolls, C.; Venkataraman, L.; Solomon, G. C. Comprehensive Suppression of Single-Molecule Conductance Using Destructive σ-Interference. *Nature* **2018**, *558* (7710), 415–419. https://doi.org/10.1038/s41586-018-0197-9.

(2) Choi, S. H.; Kim, B.; Frisbie, C. D. Electrical Resistance of Long Conjugated Molecular Wires. *Science* **2008**, *320* (5882), 1482–1486. https://doi.org/10.1126/science.1156538.

(3) Robertson, N.; A. McGowan, C. A Comparison of Potential Molecular Wires as Components for Molecular Electronics. *Chem. Soc. Rev.* **2003**, *32* (2), 96–103. https://doi.org/10.1039/B206919A.

(4) Lindsay, S. M.; Ratner, M. A. Molecular Transport Junctions: Clearing Mists. *Adv. Mater. Weinh. Ger.* **2007**, *19* (1), 23–31.

(5) Wang, W.; Lee, T.; Reed, M. A. Mechanism of Electron Conduction in Self-Assembled Alkanethiol Monolayer Devices. *Phys. Rev. B* **2003**, *68* (3), 035416. https://doi.org/10.1103/PhysRevB.68.035416.
(6) Magoga, M.; Joachim, C. Minimal Attenuation for Tunneling through a Molecular Wire. *Phys. Rev. B* **1998**, *57* (3), 1820–1823. https://doi.org/10.1103/PhysRevB.57.1820.
(7) Segal, D.; Nitzan, A.; Ratner, M.; Davis, W. B. Activated Conduction in Microscopic Molecular Junctions. *J. Phys. Chem. B* **2000**, *104* (13), 2790–2793. https://doi.org/10.1021/jp994296a.
(8) Hines, T.; Diez-Perez, I.; Hihath, J.; Liu, H.; Wang, Z.-S.; Zhao, J.; Zhou, G.; Müllen, K.; Tao, N. Transition from Tunneling to Hopping in Single Molecular Junctions by Measuring Length and Temperature Dependence. *J. Am. Chem. Soc.* **2010**, *132* (33), 11658–11664. https://doi.org/10.1021/ja1040946.
(9) Lu, Q.; Liu, K.; Zhang, H.; Du, Z.; Wang, X.; Wang, F. From Tunneling to Hopping: A Comprehensive Investigation of Charge Transport Mechanism in Molecular Junctions Based on Oligo(p-Phenylene Ethynylene)s. *ACS Nano* **2009**, *3* (12), 3861–3868. https://doi.org/10.1021/nn9012687.
(10) Choi, S. H.; Risko, C.; Delgado, M. C. R.; Kim, B.; Brédas, J.-L.; Frisbie, C. D. Transition from Tunneling to Hopping Transport in Long, Conjugated Oligo-Imine Wires Connected to Metals. *J. Am. Chem. Soc.* **2010**, *132* (12), 4358–4368. https://doi.org/10.1021/ja910547c.
(11) Capozzi, B.; Dell, E. J.; Berkelbach, T. C.; Reichman, D. R.; Venkataraman, L.; Campos, L. M. Length-Dependent Conductance of Oligothiophenes. *J. Am. Chem. Soc.* **2014**, *136* (29), 10486–10492. https://doi.org/10.1021/ja505277z.
(12) Sedghi, G.; García-Suárez, V. M.; Esdaile, L. J.; Anderson, H. L.; Lambert, C. J.; Martín, S.; Bethell, D.; Higgins, S. J.; Elliott, M.; Bennett, N.; Macdonald, J. E.; Nichols, R. J. Long-Range Electron Tunnelling in Oligo-Porphyrin Molecular Wires. *Nat. Nanotechnol.* **2011**, *6* (8), 517–523. https://doi.org/10.1038/nnano.2011.111.
(13) Bâldea, I. Protocol for Disentangling the Thermally Activated Contribution to the Tunneling-Assisted Charge Transport. Analytical Results and Experimental Relevance. *Phys. Chem. Chem. Phys.* **2017**, *19* (19), 11759–11770. https://doi.org/10.1039/C7CP01103B.
(14) Li, H. B.; Tebikachew, B. E.; Wiberg, C.; Moth-Poulsen, K.; Hihath, J. A Memristive Element Based on an Electrically Controlled Single-Molecule Reaction. *Angew. Chem. Int. Ed.* **2020**, *59* (28), 11641–11646. https://doi.org/10.1002/anie.202002300.
(15) Nitzan, A. Electron Transmission Through Molecules and Molecular Interfaces. *Annu. Rev. Phys. Chem.* **2001**, *52*, 681–750.
(16) Xu, B.; Tao, N. J. Measurement of Single-Molecule Resistance by Repeated Formation of Molecular Junctions. *Science* **2003**, *301* (5637), 1221–1223.
(17) Huang, B.; Liu, X.; Yuan, Y.; Hong, Z.-W.; Zheng, J.-F.; Pei, L.-Q.; Shao, Y.; Li, J.-F.; Zhou, X.-S.; Chen, J.-Z.; Jin, S.; Mao, B.-W. Controlling and Observing Sharp-Valleyed Quantum Interference Effect in Single Molecular Junctions. *J. Am. Chem. Soc.* **2018**, *140* (50), 17685–17690. https://doi.org/10.1021/jacs.8b10450.
(18) Yan, F.; Chen, F.; Wu, X.-H.; Luo, J.; Zhou, X.-S.; Horsley, J. R.; Abell, A. D.; Yu, J.; Jin, S.; Mao, B.-W. Unique Metal Cation Recognition via Crown Ether-Derivatized Oligo(Phenyleneethynylene) Molecular Junction. *J. Phys. Chem. C* **2020**, *124* (16), 8496–8503. https://doi.org/10.1021/acs.jpcc.9b11908.

(19) Wu, X.-H.; Chen, F.; Yan, F.; Pei, L.-Q.; Hou, R.; Horsley, J. R.; Abell, A. D.; Zhou, X.-S.; Yu, J.; Li, D.-F.; Jin, S.; Mao, B.-W. Constructing Dual-Molecule Junctions to Probe Intermolecular Crosstalk. *ACS Appl. Mater. Interfaces* **2020**, *12* (27), 30584–30590. https://doi.org/10.1021/acsami.0c01556.
(20) Wold, D. J.; Frisbie, C. D. Formation of Metal−Molecule−Metal Tunnel Junctions: Microcontacts to Alkanethiol Monolayers with a Conducting AFM Tip. *J. Am. Chem. Soc.* **2000**, *122* (12), 2970–2971. https://doi.org/10.1021/ja994468h.
(21) van Zalinge, H.; Schiffrin, D. J.; Bates, A. D.; Starikov, E. B.; Wenzel, W.; Nichols, R. J. Variable-Temperature Measurements of the Single-Molecule Conductance of Double-Stranded DNA. *Angew. Chem. Int. Ed. Engl.* **2006**, *45* (33), 5499–5502.
(22) Kamenetska, M.; Widawsky, J. R.; Dell'Angela, M.; Frei, M.; Venkataraman, L. Temperature Dependent Tunneling Conductance of Single Molecule Junctions. *J. Chem. Phys.* **2017**, *146* (9), 092311. https://doi.org/10.1063/1.4973318.
(23) Haiss, W.; Van Zalinge, H.; Bethell, D.; Ulstrup, J. ; Schiffrin, D. J. ;; Nichols, R. J. Thermal Gating of the Single Molecule Conductance of Alkanedithiols. *Faraday Discuss.* **2006**, *131*, 253–264.
(24) Frisenda, R.; Perrin, M. L.; Valkenier, H.; Hummelen, J. C.; Zant, H. S. J. van der. Statistical Analysis of Single-Molecule Breaking Traces. *Phys. Status Solidi B* **2013**, *250* (11), 2431–2436. https://doi.org/10.1002/pssb.201349236.
(25) Briechle, B. M.; Kim, Y.; Ehrenreich, P.; Erbe, A.; Sysoiev, D.; Huhn, T.; Groth, U.; Scheer, E. Current–Voltage Characteristics of Single-Molecule Diarylethene Junctions Measured with Adjustable Gold Electrodes in Solution. *Beilstein J. Nanotechnol.* **2012**, *3* (1), 798–808. https://doi.org/10.3762/bjnano.3.89.
(26) Beebe, J. M.; Kim, B.; Frisbie, C. D.; Kushmerick, J. G. Measuring Relative Barrier Heights in Molecular Electronic Junctions with Transition Voltage Spectroscopy. *ACS Nano* **2008**, *2* (5), 827–832. https://doi.org/10.1021/nn700424u.
(27) Selzer, Y.; Cabassi, M. A.; Mayer, T. S.; Allara, D. L. Thermally Activated Conduction in Molecular Junctions. *J. Am. Chem. Soc.* **2004**, *126* (13), 4052–4053. https://doi.org/10.1021/ja039015y.
(28) Lovat, G.; Choi, B.; Paley, D. W.; Steigerwald, M. L.; Venkataraman, L.; Roy, X. Room-Temperature Current Blockade in Atomically Defined Single-Cluster Junctions. *Nat. Nanotechnol.* **2017**, *12* (11), 1050–1054. https://doi.org/10.1038/nnano.2017.156.
(29) Beenakker, C. W. J. Theory of Coulomb-Blockade Oscillations in the Conductance of a Quantum Dot. *Phys. Rev. B* **1991**, *44* (4), 1646–1656. https://doi.org/10.1103/PhysRevB.44.1646.
(30) Gehring, P.; Thijssen, J. M.; van der Zant, H. S. J. Single-Molecule Quantum-Transport Phenomena in Break Junctions. *Nat. Rev. Phys.* **2019**, *1* (6), 381–396. https://doi.org/10.1038/s42254-019-0055-1.
(31) Andres, R. P. ; Bein, T.; Dorogi, M.; Feng, S.; Henderson, J. I. ; Kubiak, C. P. ; Mahoney, W.; Osifchin, R. G. ;; Reifenberger, R. "Coulomb Staircase" at Room Temperature in a Self-Assembled Molecular Nanostructure. *Science* **1996**, *272*, 1323–1325.
(32) Fan, F.-R. F.; Bard, A. J. An Electrochemical Coulomb Staircase: Detection of Single Electron-Transfer Events at Nanometer Electrodes. *Science* **1997**, *277*, 1791–1793.

For Table of Contents Only